Hygrothermal behavior of wood fiber insulation, numerical and experimental approach

Mounir Asli, Emilio Sassine, Franck Brachelet, Emmanuel Antczak

Hygrothermal behavior of wood fiber insulation, numerical and experimental approach

M. Asli[a], E. Sassine[b*], F. Brachelet[a], E. Antczak[a]

[a] Univ. Artois, ULR 4515, Laboratoire de Génie Civil et géo- Environnement (LGCgE), F-62400 Béthune, France

[b] Lebanese University, Habitat and Energy Unit, Group of Thermal and Renewable Energies - Laboratory of Applied Physics (LPA-GMTER), Faculty of Sciences, Fanar Campus, Lebanon

*Corresponding authors. E-mail address: emilio.sassine@gmail.com
mounir.asli.gc@gmail.com

Abstract

Many new insulation materials are being developed and thermally tested aiming at understanding and improving their insulation characteristics in order to improve the energy performance of new and existing buildings. Bio-sourced materials appear among the new insulation solutions presenting the advantage of being able to save energy on one hand and having a low environmental impact on the other. The wood fiber material is one of the most successful natural insulation materials being recently used in building constructions. It presents many advantages besides its insulation performance; due to its density, it stores moisture thereby improving the indoor air quality; it is also an excellent acoustic insulator because it has a natural tendency to absorb and reduce sounds.

In order to evaluate its effectiveness in building applications, this study analyzes the hygrothermal modelling and performance of the wood fiber insulation in building applications by adopting two approaches:

- A numerical approach using a mathematical model that describes heat and mass transfer within the wood fiber material being considered as porous media. The hygrothermal characteristics of the wood fiber material are first determined experimentally for this purpose, namely the thermal conductivity, the heat capacity, and the isotherms of sorption and desorption.
- An experimental approach is carried out in controlled and uncontrolled ambiance conditions in order to validate the numerical model.

A 50 cm x 50 cm wood fiber sample having an 8 cm thickness is tested for this purpose. A very high accordance is observed between the measured and modelled results for both the temperature and the relative humidity evolutions within the sample at x=2cm and x=4cm with a mean difference $\overline{\Delta T}$ of

0,21°C at x = 4cm and 1°C at x = 2cm. The maximum recorded differences for the relative humidity are: 5,5% and 4,5% at x = 2cm and 4 cm respectively.

The ability to predict the thermal and the hygric behavior of the wood fiber insulation will thus allow a better understanding of the efficiency of natural insulation materials.

Keywords —

Wood fiber, hygrothermal behavior, experimental and numerical study, isotherm of sorption, thermal conductivity.

Nomenclature

D_T	Mass transport coefficients associated to temperature gradient ($m^2.s^{-1}.K^{-1}$)
D_θ	Mass transport coefficients associated to moisture gradient ($m^2.s^{-1}$)
ρ_0	Solid matrix density (kg/m^3)
L_v	Latent vaporization heat ($kJ.kg^{-1}$)
ρ_l	Water density ($kg.m^{-3}$)
Cp_m	Average specific heat ($J.kg^{-1}.K^{-1}$)
λ*	Equivalent thermal conductivity ($W.m^{-1}.K^{-1}$)
T	Temperature (°C)
RH	Relative humidity (%)
t	Time (s)
δ_0	Water vapor permeability ($kg.m^{-1}.s^{-1}.Pa^{-1}$)
δ_a	Air vapor permeability ($kg.m^{-1}.s^{-1}.Pa^{-1}$)
ξ	Specific hygric capacity ($kg.m^{-3}$)
μ	Water vapor resistance factor (-)

1 Introduction

Nowadays, human activities are causing the depletion of natural resources and significant climate changes impacting the environment through the increasing occurrence of natural disasters such as floods, hurricanes, drought, and heatwaves…etc. In order to deal with these issues, the international community is seriously concerned trying to reduce the greenhouse gas emissions (GHG) by 2050 across the globe [1], [2]. While developing countries are unable to meet the highly fixed objectives, the industrialized countries are in turn making a special effort to divide by four their GHG in less than fifty years without compromising a sustainable development of their societies.

The building sector is particularly involved in such commitments. In France, as in many other countries, the building sector is the largest energy consumer among all economic sectors with about 43% of the global consumed energy (1.1 ton oil equivalent per year per capita according to the ADEME [3]). Moreover, the buildings produce over 120 million tons of carbon dioxide and greenhouse gases representing nearly a quarter of national emissions [4]. Furthermore, the cost of energy bills alone accounts for 30% of the household budget; and these figures are expected to increase due to the decrease of fossil fuel availability in the coming years [5]. Substantial efforts are thus required for improving the energy performance of both new construction and existing buildings [6]. These efforts will not only reduce the energy cost, but also improve the well-being of residents by improving the indoor thermal comfort; as well as providing employment opportunities in the building sector [7].

The choice of building materials is just as important as good design and quality construction. They have a significant impact on the energy bill [8], [9]. However, the energy required for their production, transportation, implementation and recycling should be taken into consideration. It is therefore wise to look for the usage of natural materials having equivalent performance and reduced environmental impact compared to those produced by chemical processes.

Bio-based materials are by definition the materials made from plant biomass resources or animal origins. They now cover a wide range of products and are used in many applications in the building and construction field such as bricks [10], insulations (wool plant or animal fibers, recycled textiles, cellulose wadding, straw bales, etc.), mortars and concretes (hemp concrete, wood, flax, etc.) [11], [12], and panels (particles or plant fibers, compressed straw, etc.) [13], [14].

This study investigates the hygrothermal performance wood fiber materials. These products are manufactured on the basis of shredder softwood falls and present considerable environmental advantages, because they use wood being a natural and renewable resource that can be obtained from recycling the wastes from the timber industry.

The wood fiber materials can be found in various forms: Panels with a density of 40 $kg.m^{-3}$ known as semi-rigid wood fiber panels. These are usually elastic, flexible and easily adaptable. They are generally used as interior insulation. The timber fiberboards panels are rigid with medium or high density (between 60 and 280 $kg.m^{-3}$ or more), are mainly used in roof insulation and outside wall insulation. The wood fiber bulk material has a density of 35 $kg.m^{-3}$ and is collected just after the shredding step; it can be blown or projected by inside. They can also be mixed with clay or concrete as innovative insulation material ~~[11]~~ [15].

The use of bio-based material in building insulation is not limited to its advantageous thermal performance, but also to its sensitivity to moisture, in other words its ability to absorb and desorb water vapor in real weather conditions [16]. Indeed, in new construction or in existing buildings' rehabilitation, the moisture can be present in the walls under several forms such as: water vapor coming from inside, capillary water rise, exposure to weather conditions, etc… Moreover, by their nature, the bio-based materials are quite sensitive to the water and water vapor presence [17], [18], which obviously impacts their durability and thermal performance.

In industrialized countries, the implementation of bio-based materials in building construction is recent and is still limited.

Many research works investigated the thermal behavior of wood fiber construction materials. Troppova et al. [19], determined the thermal properties of medium density fiberboards with different thicknesses using a transient method. El-Sawalhi et al. [20], examined the structure and the thermal performance of natural fiber insulation materials through 3D tomographic imaging by measuring critical structural parameters like porosity, pore and fiber size distribution as well as local fiber orientation distribution. Even though these studies present interesting findings for understanding the thermal behavior of wood fiberboards, the importance of mass transfer in these porous materials was not taken into consideration.

Among the studies dealing with heat and mass coupling in wood fibers, Mvondo et al. [21], studied the influence of water content and the direction of the fibers on thermophysical properties for three tropical wood species by determining experimentally the thermal conductivity and volumetric heat capacity in the longitudinal, radial and tangential directions of the different samples for different moisture contents. The study presents interesting results helping to understand the relation between thermal and hydric properties in fibrous materials. Latif et al. [22] compared Mineral Wool, Wood Fiber and an assembly of wood fiber and hemp-lime panels having identical U-values in a large dual environmental chamber under identical controlled conditions. It was observed that the wood fiber and hemp-lime assembly panel showed the highest heat storing and releasing capability as well as the highest moisture dampening ability which can be useful in mitigating overheating of dwellings and reducing interstitial condensation. The effect of adding inorganic adsorbents was studied by Nguyen et al. [23] who found that they lead to a decrease in the thermal conductivity and an improvement in the moisture buffering of the insulation boards.

In this same approach, this work aims to study the wood fiber insulation, by analyzing its transient hygrothermal behavior and evaluating these intrinsic characteristics, which are temperature and moisture functions. For this reason, the present study is made of two parts:

- First, an adapted behavior pattern to predict the hygrothermal behavior of wood fibers is proposed using a mathematical model based on Philip and De Vries model [16]. A thermophysical characterization study is performed according to the standards for determining the material thermophysical properties.

- Then, the numerical model is validated through experimental results on a wood fiber wall submitted to controlled and uncontrolled ambient solicitations.

A comparative study of the decrement factor and time lags is also provided, and a comprehensive sensitivity analysis is presented in order to evaluate the results and the accuracy of the model.

2 Numerical heat and mass coupled model

2.1 Governing equations

Several models were carried out to investigate the coupled heat and mass transfer in porous media. The most popular ones are Philip and De Vries model [24] Whitaker [25] and Luikov [26]. Two approaches are generally used:

The first one is based on the homogenization of the porous media at microscopic and macroscopic scale. The porous media that is highly heterogeneous at microscopic scale is represented as a homogeneous and continuous media. The heat and mass conservation is written to describe the particle movement, then the variable states are averaged over the entire volume of the domain. Whitaker [25], Samson [27] and Maghous [28] are examples of works using this approach. It allows a better understanding and modelling of the complex phenomena that occur simultaneously at the pore scale, for example the water and the water vapor diffusion.

The second approach consists on phenomenological modelling, inspired by the works of Phillipe De Vries [24] Luikov [26] Kunzel [29]. In this part the porous media is considered as continuous and homogeneous media, with equivalent properties, which allows to establish the heat and mass transfer equations from the thermodynamic principles. Most of these works are based on Fourier's heat conduction law, fluid mechanics Darcy law for fluid diffusion, and Fick's law for vapor diffusion [30]. The following assumptions are considered:

- The solid matrix is considered homogeneous, continuous and non-deformable.
- The medium volume equals at least a representative elementary volume (REV).
- The thermodynamic equilibrium is established between the different material components.
- Total gas pressure is constant, equal to the atmospheric pressure.

The model of Philip and De Vries [24] is taken as the basic model in this work for predicting the hygrothermal behavior of the wood fiber bio-based material. It takes into account moisture transport under two phases (liquid and vapor) and assumes that the vapor phase moves under a gradient of partial vapor pressure and the water phase moves under capillarity. With these considerations, the heat conservation equation becomes:

$$\rho_0 \, Cp_m \, \frac{\partial T}{\partial t} = \frac{\partial}{\partial x}\left(\lambda^* \, \frac{\partial T}{\partial x}\right) + \rho_l \, L_v \left(\frac{\partial}{\partial x} D_{T,v} \, \frac{\partial T}{\partial x}\right) + \rho_l \, L_v \frac{\partial}{\partial x}\left(D_{\theta,v} \cdot \frac{\partial \theta}{\partial x}\right) \quad (1)$$

Where T and θ are the temperature and water content respectively

ρ_0 is the solid matrix density

L_v is the latent vaporization heat

ρ_l is the water density

Cp_m is the specific heat calculated as the average specific heat of solid matrix and liquid phase.

λ* is the equivalent thermal conductivity of the porous media and it is a function of temperature and moisture content

$D_{T,v}$ and $D_{\theta,v}$ are the vapor phase transport coefficients associated with temperature and moisture content gradient respectively

The mass transfer balance equation is given by:

$$\frac{\partial \theta}{\partial t} = \frac{\partial}{\partial x}\left(D_\theta \frac{\partial \theta}{\partial x}\right) + \frac{\partial}{\partial x}\left(D_T \frac{\partial T}{\partial x}\right) \quad (2)$$

D_T and D_θ are, respectively, the mass transport coefficients associated with temperature and moisture content gradient.

2.2 Boundary conditions

The air velocity sensors may induce relatively high uncertainty measurements, especially at the exterior side of the wall where the ambient conditions may be very disturbed. The convective heat and mass transfer at the air–porous material interfaces [31] may generate some uncertainties in the numerical modelling; imposed temperature and relative humidity on the internal and external wall sides were thus considered as boundary conditions for the numerical model (Dirichlet type boundary conditions).

The relative humidity and temperature sensors were placed at the internal and external faces of the wall, and the Dirichlet type boundary conditions can be written as:

$$T_{sext,t} = \mathrm{T}_{ext} \ , \qquad T_{sint,t} = \mathrm{T}_{int} \quad (3)$$

$$HR_{sext,t} = \mathrm{HR}_{ext} \ , \qquad HR_{sint,t} = \mathrm{HR}_{int} \quad (4)$$

Where the indices “sext” and “sint”, represent the temperature and humidity at the interior and exterior wall surfaces respectively, and “t” refers to the dynamics of the variables as a function of time.

To be closer to the reality, the temperature and relative humidity at the boundaries were measured during the tests.

2.3 Diffusion coefficients

The equations relating mass transport coefficients to vapor and liquid phase transport coefficients are:

$D_T = D_{T,l} + D_{T,v}$ $\quad m^2.s^{-1}.K^{-1}$ (5)

$D_\theta = D_{\theta,l} + D_{\theta,v}$ $\quad m^2.s^{-1}$ (6)

The vapor diffusion coefficients were determined according to Zeknoun et al [32], and Maalouf et al [33]. The transport coefficients associated with moisture gradient are related to the water vapor permeability δ_0 and the specific hygric capacity ξ, which is the slope of sorption curve:

$$D_\theta = \frac{\delta_0 \ P_{v,s}}{\rho_0} \ \frac{1}{\xi} \quad (7)$$

$$\delta_0 = \frac{\delta_a}{\mu} \quad (8)$$

Where δ_a is the air vapor permeability and it is equal to 2.10^{-10} $kg.m^{-1}.s^{-1}.Pa^{-1}$, and μ is the water vapor resistance factor.

Vapor transport coefficient under a temperature gradient is given by the relation:

$$D_{T,v} = \frac{\delta_0 \ \varphi}{\rho_l} \ \frac{dP_{v,s}}{dT} \quad (9)$$

2.4 Numerical resolution

To solve the model of heat and mass transfer represented by Eq. (1) and Eq. (2), Comsol Multiphysics® software [34] was used. The software is adapted to solve partial differential equations, based on the finite elements method (FEM) especially in Multiphysics problems where several coupled phenomena occur simultaneously. The specific boundary conditions of heat and mass flux represented in Eq. (3) and Eq. (4) have been implemented. Several simulations were done in order to determine the effect of the mesh on the accuracy of the results, and to be as confident as possible, it has been decided to tighten the mesh to the maximum so that the mesh length is 0.02mm with a 300s time step. The value settings of the parameters used in the numerical simulations are summarized in Tab. 1.

Tab 1. Parameters value settings

Parameter	Value	Reference
ρ_0	187 (kg.m^{-3})	Measured
L_v	2454 (kJ.kg^{-1})	[35]
ρ_l	1000 (kg.m^{-3})	Fundamental constant
Cp_m	Results in Fig. 4-b	Measured
λ*	5E^{-05}(w^2) + 0.0002(w) + 0.0437	Measured
δ_a	2.10^{-10} (kg.m^{-1}.s^{-1}.Pa^{-1})	[36]
ξ	Results in Fig. 2	Measured
μ	3 (-)	[36]

3 Experimental characterization of wood fiber

The wood fiber materials hold very interesting properties related to their hygrothermal performance, represented by their low thermal conductivity [37] [38] and their high hygroscopic properties of humidity buffering [36]. Several works have been carried out to characterize wood fiber materials such as the work of Vololonirina and al. [36] studying the impact of moisture on the wood fiber product properties and the experimental study of Rafidiarison and al. [16] investigating the heat and mass transfer within the wood fiber insulation panels with different wall configurations and different boundary conditions.

3.1 Adsorption and desorption of wood fiber

In this work, a series of characterization tests was established in our laboratory to guarantee the accuracy of the parameters used in the numerical model describing the hygrothermal behavior of wood fiber. Water vapor sorption is the process [39] that relates the water content inside the materials with the ambient relative humidity, for a given temperature. The porous materials with open porosity tend to fix the air humidity, which means the increase in air relative humidity leads to an increase of bulk

density and vice versa. Generally, in order to classify the isothermal sorption of porous materials, the classification of the International Union of pure and Applied Chemistry (IUPAC) [40] is adopted. Note that the water content quantities at the sorption state differ from the quantities evaluated at the desorption [41].

3.1.1 *Experimental setup*

The water vapor sorption and desorption test was performed according to the discontinuous method described in the standard NF EN ISO 12571 [42]. The dynamic VDS test method was used where the ambient conditions are ensured by mechanical ventilation system. Three samples were tested for the wood fiber, which is the minimum required number by the standard NF EN ISO 12571 [42]. The three samples were placed inside a climatic chamber, where the climatic ambient conditions (temperature and relative humidity) were controlled. The wide range of temperature (-40°C to 60°C) and relative humidity (0% and 97%), allows reproducing the test conditions with high flexibility. The uncertainties in temperature and relative humidity were evaluated by the supplier at 0.5°C and 2% respectively. The water content was determined for successive stages of relative humidity (increasing then decreasing) for a constant temperature 23°C (isothermal condition).

The samples were weighted until reaching the steady state; when a mass difference lower than 0.1% was reached after three successive weights in 24h, the equilibrium was considered to be reached, and the water content was calculated according to Eq. 10.

$$\theta = \frac{m_0 - m}{m_0} \qquad (10)$$

Where m_0 is the mass of the sample in the dry state and m is the mass sample of the steady state.

Fig. 1 shows the kinetic sorption of wood fiber for different humidity stages [0%, 10%, 23%, 55%, 81%, 90% and 97%] for sorption and [97%, 90%, 81%, 55%, 23%, 10% and 0%] for desorption.

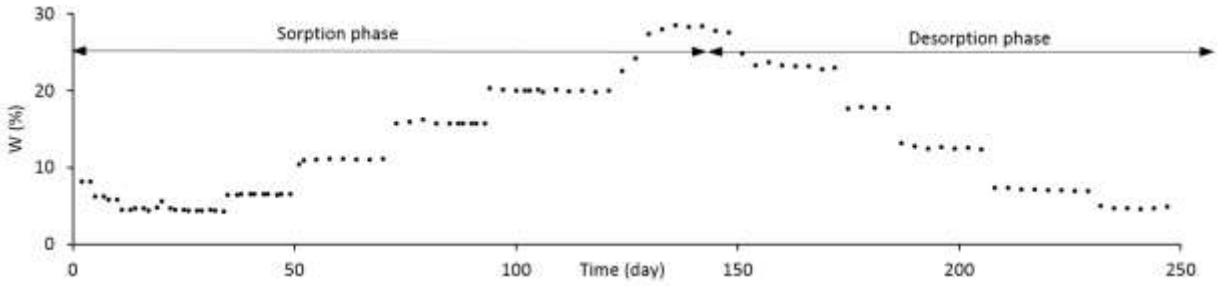

Figure 1- Kinetic sorption isotherm of wood fiber

3.1.2 *Sorption Modelling*

The purpose of the isotherm modelling is to have the water content curve spread out over the relative humidity range φ (1 to 100%). Several models have been developed to fit the sorption curve; the empirical formulations with the most accuracy are: the Langmuir model [43], the GAB model developed by (Guggenheim [44] Anderson [45] and De Boer [46]) and the BET model [47]; the equations of these models are listed in Tab. 2.

Tab 2. Sorption models.

Models	Equations
Langmuir	$w = \theta_m + \frac{C.\varphi}{1 + C.\varphi}$
BET	$w = \frac{C.\theta_m.\varphi}{(1-\varphi).(1-\varphi+C.\varphi)}$
GAB	$w = \frac{C.\theta_m.K.\varphi}{(1-K.\varphi).(1-K.\varphi+K.C.\varphi)}$

w is the water content of the material on a dry basis (kg water / kg dry solid)

θ_m is the water content corresponding to the monolayer sorption for each model

$\varphi = (P_v/P_s)$ is the water activity

P_v and P_s are respectively the vapor partial pressure and saturation pressure

C and K are constants related to the temperature effect.

$C = exp^{\frac{E_a - E_m}{R.T}}$ $K = exp^{\frac{E_l - E_m}{R.T}}$

E_a is the heat of adsorption, E_l is heat liquefaction, and E_m is binding energy.

The GAB model was compared to the obtained results of the water vapor sorption test since it covers a wide range of relative humidity ($0.05 < \varphi < 0.95$), while the other models cover a narrower range.

In order to obtain the different GAB model parameters, the least-square method was being implemented:

$$\sum(w_i - w_{exp,i}) = \text{minimum} \quad (11)$$

$w_{exp,i}$ is the water content measured at the relative humidity i, and w_i is water content calculated by the GAB model.

The relative error of linear regression can be calculated as:

$$E = \frac{1}{n}\sum_{i=1}^{n}\frac{abs\,(w_i - w_{exp,i})}{w_{exp,i}} \quad (12)$$

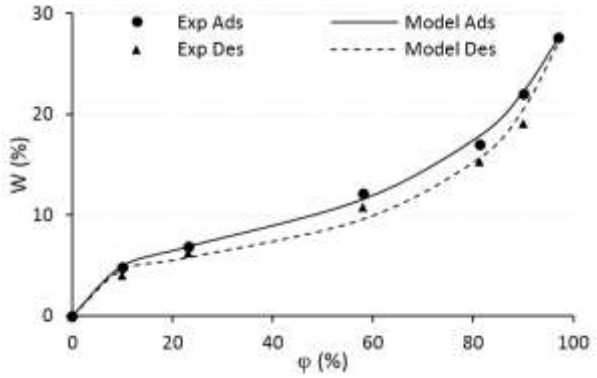

Figure 2- Adsorption and Desorption curve of wood fiber

Fig. 2 shows the experimental and fitting sorption isotherm curves for the wood fiber. According to the IUPAC classification **[40]** the tested material can be classified as type II, which is of sigmoid format. This type of curve is obtained for the micro-porous media and is in accordance with the nature of wood fiber. Furthermore, the sorption isotherm presents a hysteresis, which extends to the lower hygrometry. From this curve, three segments of the water content evolution can be observed, the test started from 0% of water content, which is the initial condition assumed (dry material). The first part at lower relative humidity $\varphi < 23\%$, less than 5% of water content is recorded, only a monolayer is formed. The second part, $23\% < \varphi < 80\%$, the water content presents a slight slope. The last part, at high hygroscopic region, $80\ \% < \varphi < 97\ \%$, the moisture inside pores begins to form a water bridge, which is known as the condensation phenomenon. Tab. 3 summarizes the measurements of water content and their corresponding relative humidity, for both adsorption and desorption stages. The hysteresis is represented by the ratio between the average values obtained for adsorption and desorption (A/D).

Tab 3. Water content versus relative humidity.

RH %		0	10	23	58	81	90	97
Wood fiber	**Ads**	**0**	**4.12**	**6.34**	**10.82**	**15.32**	**19.02**	**27.74**
	Des	**0**	**4.81**	**6.93**	**12.27**	**17.11**	**22.09**	**27.74**
	A/D		**0.85**	**0.91**	**0.88**	**0.89**	**0.86**	**1**

The fitted parameters of the GAB model, namely the monomolecular water content θ_m, and the energy values (C and K) are given in Tab. 4. The obtained results present a big similarity with the work of Vololonirina and all **[36]** for the isotherm of sorption data.

Tab 4. Fitted parameters for the GAB model

Materials	C (-)	K (-)	θ_m (kg/kg)

Wood Fiber	**Ads**	**55.730**	**0.841**	**0.0500**
	Des	**26.800**	**0.788**	**0.0655**

3.2 Thermal characterization

3.2.1 Experimental method

Thermal characterization techniques were based on the study of the response of a sample material to a thermal loading. The guarded hot plate and heat flow meter methods according to the standard NF EN 822 [39] were used to measure thermal conductivity and specific heat of the tested material. This method was adopted due to its simplicity and its results' accuracy.

The experimental setup consists of maintaining a temperature difference ΔT between two parallel flat plates, a sample with known thickness (*e=8cm*) is positioned between them. The sample's area was selected higher than the flux sensor' area (15 cm x 15 cm) in order to prevent border heat loss effect. Fig. 3 shows a schematic of the principle and the tested specimen.

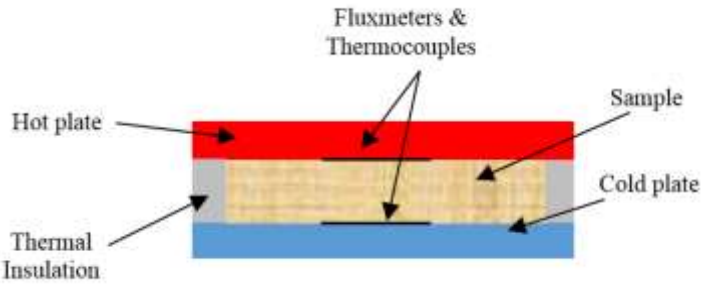

Figure 3- Schematic of principle heat flow meter method

The thermal conductivity λ can calculated as follow:

$$\lambda = \frac{e \,.\, \Phi}{\Delta T} \tag{13}$$

Where λ ($W.m^{-1}.K^{-1}$) is the material's thermal conductivity, and Φ ($W.m^{-2}$) is the measured heat flux.

Likewise, the specific heat was evaluated with the same device using different imposed thermal loads. The sample was first submitted to a constant temperature until reaching a steady-state, then another constant temperature was applied until reaching a new steady-state. We assume that the sample goes from initial temperature T_{init} to final temperature T_{fin}. Between these instances the sample stores an amount of energy Q ($J.m^{-2}$); the heat capacity C ($J.K^{-1}.m^{-2}$) is thus calculated as follows:

$$C = \frac{Q}{\Delta T} \tag{14}$$

Where $\Delta T = T_{fin} - T_{init}$, and $Q = \int_{T_{init}}^{T_{fin}} \Delta\Phi . dT$

The specific heat c ($J.K^{-1}.Kg^{-1}$):

$$c = \frac{C}{\rho \,.\, A \,.\, e} \tag{15}$$

Where ρ and e are the material density and thickness respectively.

3.2.2 *Experimental results*

The thermal and hygroscopic characteristics of materials were tested in laboratory as described below. The wood fiber material is first dried at constant temperature 100°C during 48h, then the thermal conductivity and heat capacity were measured. Afterwards, the sample was placed inside a climatic chamber and submitted to different relative humidity conditions. The water content was determined for each state and the thermal characteristics were measured for each corresponding water content. Fig. 4a represents the thermal conductivity evolution versus water content of wood fiber material. We observe a parabolic curve that represents the thermal conductivity evolution, where the lowest value corresponds to the dry thermal conductivity λ_0 = 0.044 $W.m^{-1}.K^{-1}$. The measured λ_0 is in accordance with the value founded by Vololonirina et all [36]. However, the wet thermal conductivity reaches 0.063 $W.m^{-1}.K^{-1}$ when the sample contains 20% of water content. The thermal conductivity presents a 43% growth compared to the initial measured value at the dry state, this shows the great influence of water content on the thermal behavior of wood fiber. The fitting curve relating the thermal conductivity of wood fiber to its water content is given by:

$$\lambda_{wood\ fiber} = 5E^{-05}(w^2) + 0.0002(w) + 0.0437 \quad (16)$$

The volumetric heat capacity of wood fiber (ρ.c) $J.m^{-3}.K^{-1}$ as a function of water content was determined by the same method (Fig. 4b). The relationship between the volumetric heat of wood fiber and water content presents a linear shape and can be expressed as:

$$\rho.c_{\ wood\ fiber} = 8051.2(w) + 250132 \quad (17)$$

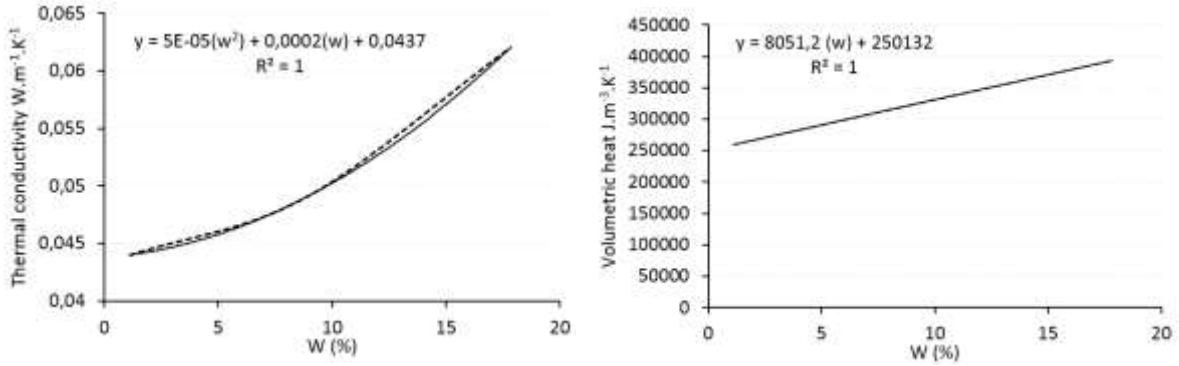

(a) (b)

Figure 4- Thermal conductivity (a) and volumetric heat capacity (b) versus water content of wood fiber

The vapor permeability test (dry-wet cup [49]), requires a specific set-up and takes a long time to be performed adequately, for these reasons the water vapor permeability values of studied materials were taken from the literature [36] [50].

4 Controlled conditions test

4.1 Experimental setup

The wood fiber material sample was first exposed to controlled temperature and humidity boundary conditions inside the previously described climatic chamber. The sample has a 300mm x 300mm open section and is 80mm thick. To ensure a 1-D heat and mass transfer within tested sample, only the two large faces were exposed to the ambient conditions, the other faces being insulated with polyurethane and a vapor-tight material (silicone). A controller device was used to monitor the ambient temperature and relative humidity. Two other specimens with same configuration with different thicknesses 2mm and 4mm were also placed in the climatic chamber; these samples were weighted each time to assess the water content evolution with an accuracy of ± 0.01 g.

The sample was instrumented with thermocouples and humidity sensors HIH-4000 to assess the temperature and relative humidity evolutions respectively. As shown in Fig. 5, the sensors were placed within the material thickness at different positions x = 0mm, 20mm, 40 mm and 80mm, and inside the climatic chamber in order to assess the relative humidity and temperature of the surrounding. The advantages of these sensors are their long-term stability and the fact of being individually calibrated, their accuracy is evaluated by the supplier to ± 3.5% for humidity and ± 0.02 °C for temperature. The data logging was done through a data acquisition system GL820 [51] connected to the sensors.

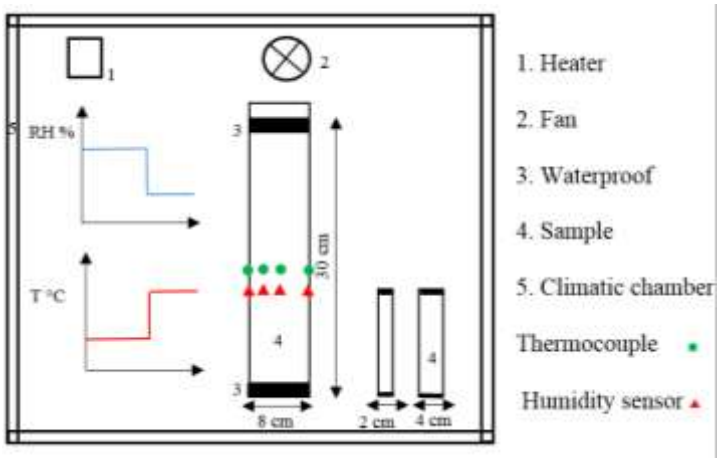

Figure 5- Schematic representation of experimental facility

4.2 Ambient conditions

The samples were first dried in a ventilated oven at 100°C in order to obtain the dry mass. They were next introduced inside the climatic chamber, where they were exposed to constant ambient conditions φ = 50% and T = 23°C for long periods. After 21 days, the samples of wood fiber were assumed to reach the steady state. The measured values were used in the modelling section as initial conditions.

Several test protocols of static solicitation have been performed inside the climatic chamber to identify precisely the relation between the temperature and relative humidity. The imposed measured ambient conditions of temperature and humidity for the three protocols are shown in Fig. 6.

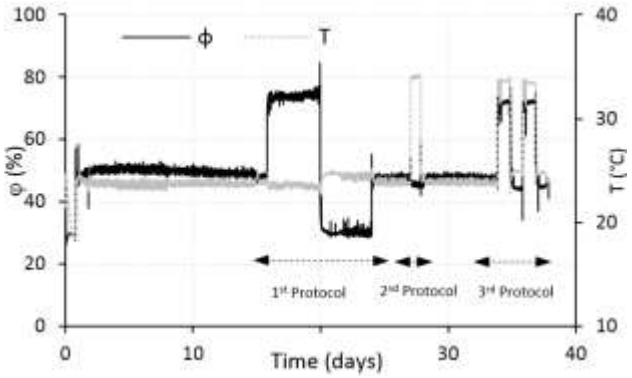

Figure 6- Static solicitation of relative humidity and temperature

The first case study (first protocol) consisted in maintaining a constant temperature (T= 24°C), while varying φ from 50% to 75% for 4 days, then switching φ to 33% for other 4 days. Then the samples were submitted to T = 24°C and φ = 50% for 5 days, in order to reproduce the initial conditions before starting the second protocol.

The second case study consisted in maintaining a constant φ at 50% and switching the temperature from 24°C to 34°C, thus imposing a 10°C temperature gradient during 1 day.

In order to test the model's ability to predict the hygrothermal behavior, the 3rd protocol was performed by coupling the ambient condition variations of the air temperature (from 24°C to 34°C), simultaneously with the humidity from (50% to 75%) during 1 day. The operation was repeated 2 times.

4.3 Experimental results

Fig. 7 – Fig. 9 show the experimental temperature and humidity measurements for the three protocols.

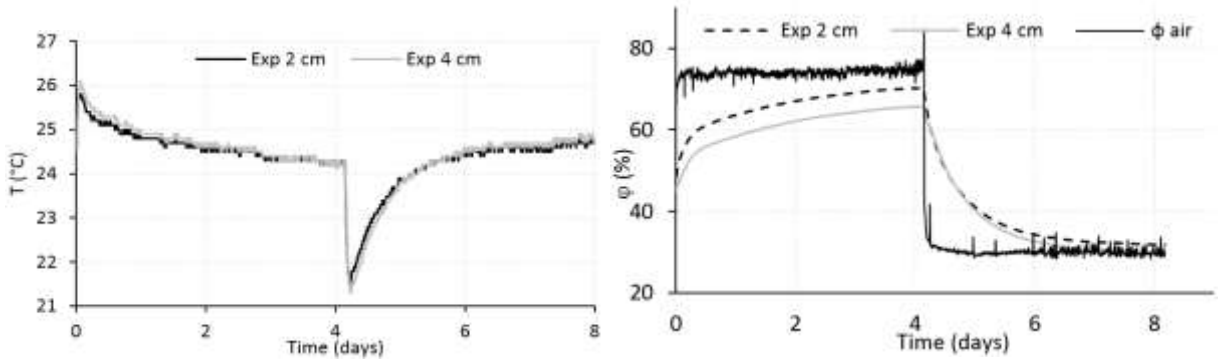

(a) (b)

Figure 7- Measured temperature (a) and relative humidity (b) evolution within sample (1st protocol)

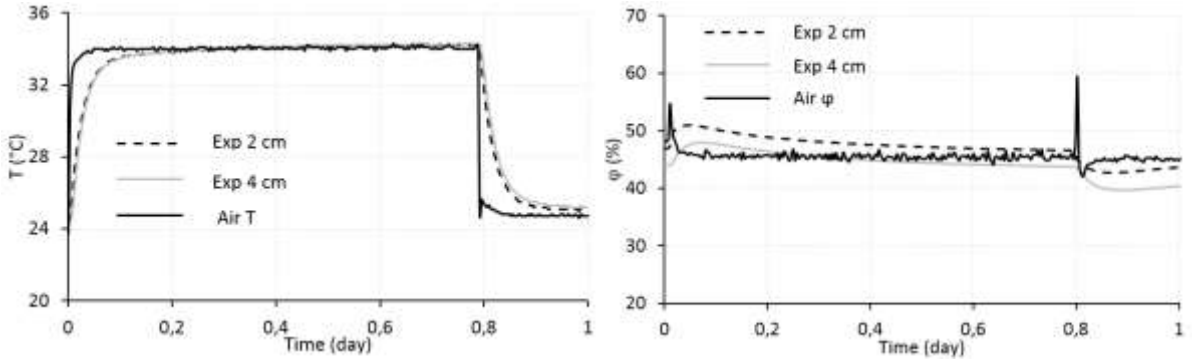

(a) (b)

Figure 8- Measured temperature (a) and relative humidity (b) evolution within sample (2nd protocol)

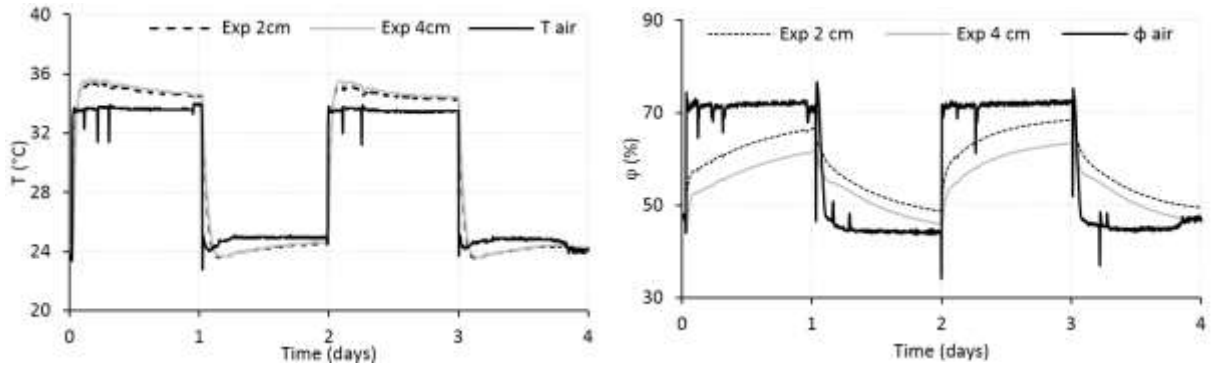

(a) (b)

Figure 9- Measured temperature (a) and relative humidity (b) evolution within sample (3rd protocol)

In the first protocol, when switching the air relative humidity φ from 50% to 75%, the quasi steady state is reached after four days, for both sorption and desorption stages (Fig. 7b). The relative humidity within the sample started evolving gradually, where the evolution at the first 12 hours was more acute; that can be explained by the monolayer adsorption phenomenon “Van der Waals forces”, which is more important than the multilayer sorption forces. During the desorption phase, the evolution of relative humidity continued, however with less emphasis. The relative humidity φ at 2cm and at 4cm reached 70.38% and 65.74% respectively for the adsorption stages, and 31.76%, 29.89% for the desorption stages respectively. It can be shown that the fiber wood behavior during adsorption and desorption stages is not similar, this is due to the pores shape. Every relative humidity variation is accompanied of temperature fluctuation (Fig. 7a), this phenomenon is caused by the coupled effect of mass on heat transfer. The condensation around the thermocouples, is characterized by latent heat liberation and for this reason the temperature peaks at t=0 and t=4days are evaluated to be about +1.5°C for the sorption stage, and -3°C for the desorption.

In the second protocol, the air temperature increases from 24°C to 34°C; as expected the air temperature reaches the steady state after a very short time (about 20 minutes). The temperature profiles at 2cm and 4cm reach the steady-state thereafter, after about 1 hour (Fig. 8a). Concerning the

relative humidity evolution during the second protocol (Fig. 8b), small peaks of relative humidity, φ: 50,92% and 47,99%, are registered at 2cm and 4cm respectively.

The third protocol is the closest to reality where temperature and relative humidity variations occur simultaneously. The air relative humidity and temperature measurements within the sample at 2cm and 4cm are shown in Fig. 9.

4.4 Comparison and discussion

The modelling was performed using COMSOL Multiphysics® in 2-D configuration with a mesh size of 1 mm and a time step of 300s; Dirichlet boundary conditions were adopted and the logged data at the interfaces were implemented in the model. The initial conditions were also taken from the measured values.

4.4.1 First protocol

The comparison between the modelled and measured relative humidity and temperature in the first protocol (Fig. 10), shows a good agreement between the experimental and the simulated data. A small difference is observed between the measured relative humidity and the modelled one in 2cm depth (Fig. 10b). The simulated temperature at 2cm and 4cm follows the temperature measured. The temperature peak is estimated to be 1.2°C and 1.5°C at 2cm and 4cm respectively during the sorption stage, and 2.5°C and 2.65°C during the desorption stage.

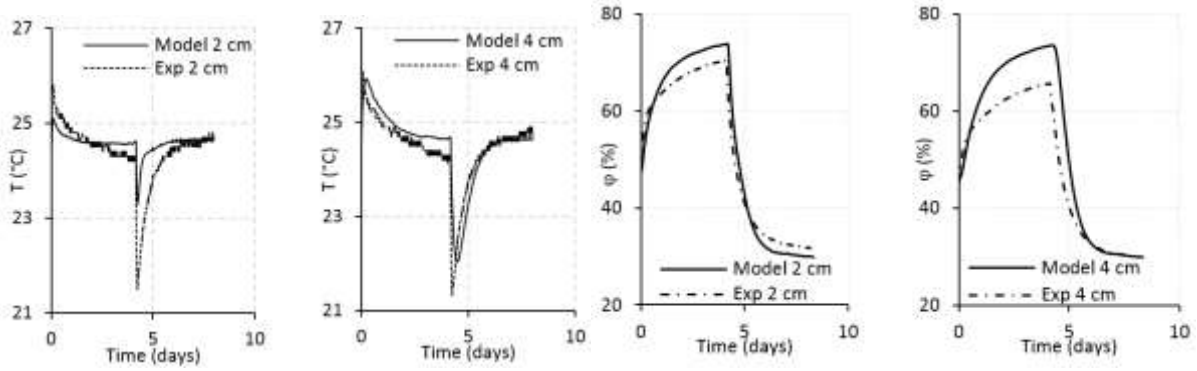

(a) (b)

Figure 10- Measured and modelled Temperature (a) and Relative humidity (b) evolution at x = 2 and 4 cm (1st protocol)

The water content is evaluated during the test, where the samples inside the climatic chamber were weighted on a regular basis. The operation is done for the 1st and the 3rd protocols, and ignored for the 2nd protocol (where the relative humidity was maintained constant). Fig. 11 represents the modelled and measured water content evolution within the sample. The measured water content starts from 7.4 kg/kg and 6.13 kg/kg at 2cm and 4cm respectively, which corresponds to the sorption curve of wood fiber (Fig. 2). The water content continues the evolution with the same way as the relative humidity, until reaching 10.15 kg/kg and 10.37 kg/kg at 2cm and 4 cm respectively. During desorption stage the water content decrease to 5.24 kg/kg and 5.09 kg/kg in four days. Hysteresis effect of 2.16 kg/kg and 1.04 kg/kg between the sorption and desorption stages at 2cm and 4cm are logged respectively. Generally, a good agreement is observed between the modelled and the measured water content; the

observed slight difference is due to the hysteresis effect, which has not been considered in the modelling part.

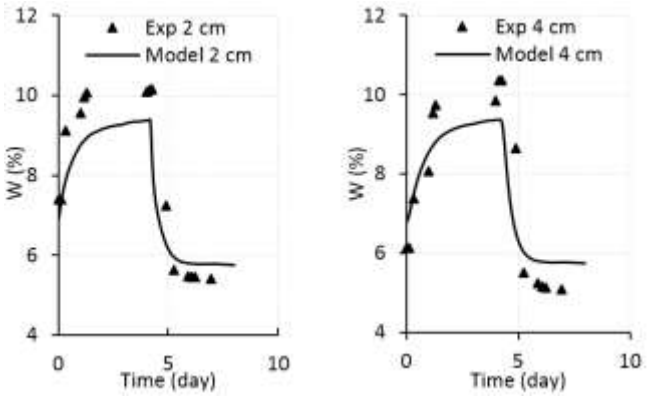

Figure 11- Measured and modelled Water content evolution at x = 2 and 4 cm (1st protocol)

4.4.2 Second protocol

In the second test where a constant relative humidity of φ = 50% was maintained while varying the temperature, the heat transfer phenomena within the wood fiber was studied without accounting the humidity effect; this allows to check the accuracy of the thermal characteristics obtained in laboratory, namely the thermal conductivity and the specific heat of wood fiber. The simulated and measured temperatures for this configuration are shown in Fig. 12. The steady state is quickly reached within the wood fiber sample and the temperature profiles at 2cm and 4cm are very similar. A good agreement is recorded between the simulated and the measured temperatures, where average temperature differences ΔT of 0.08°C and 0.13°C are evaluated at 2cm and 4 cm respectively.

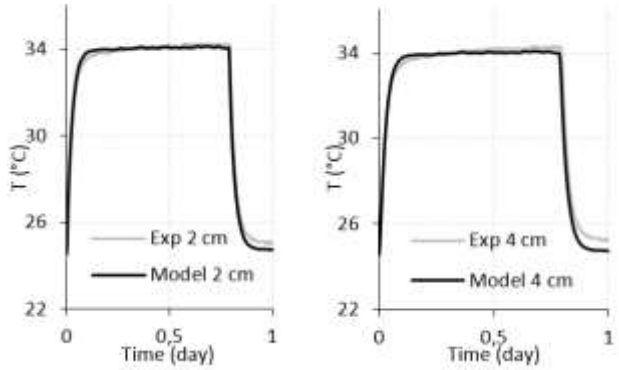

Figure 12- Measured and modelled temperature evolution at x= 2cm and 4 cm respectively (2nd protocol)

4.4.3 Third protocol

The third protocol, consisting of varying simultaneously the temperature and the relative humidity, aims at submitting the sample to a consecutive fast moisture adsorption and desorption 1 day cycles, and is repeated two times.

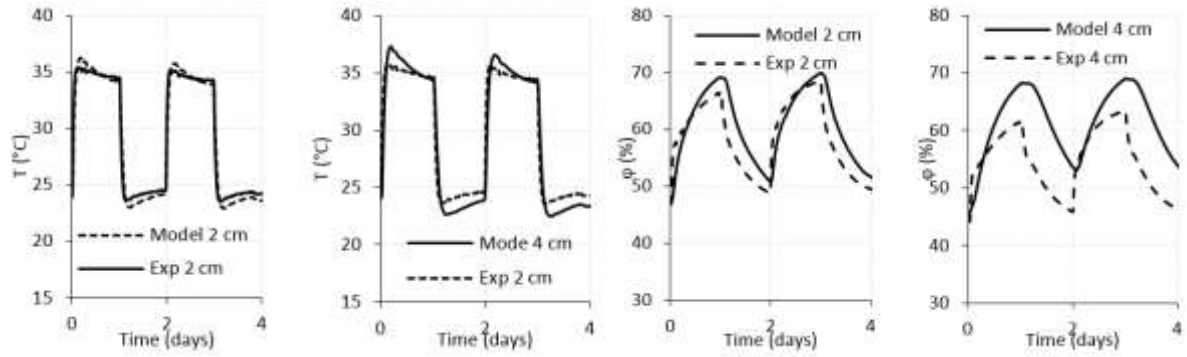

(a) (b)

Figure 13- Measured and modelled Temperature (a) and Relative humidity (b) versus time at x = 2 and 4 cm (3rd protocol)

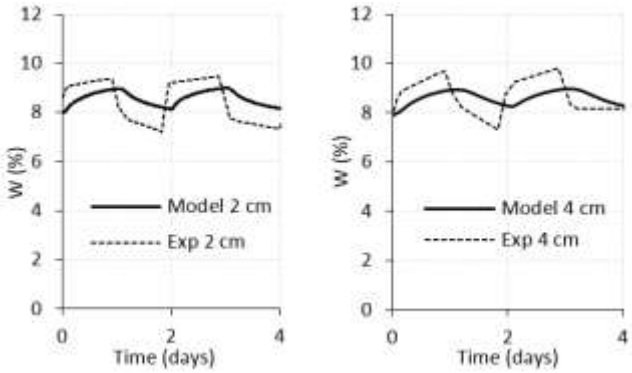

Figure 14- Measured and modelled Water content evolution versus time at x = 2 and 4 cm (3rd protocol)

The temperature evolution is predicted accurately over the entire thickness in terms of amplitude and time lags (Fig. 13a). Fig. 13b represents the numerical and experimental relative humidity evolutions within the sample at 2cm and 4cm respectively. As expected, the mass transfer process takes more time to reach the quasi steady state than the heat transfer process. A close difference between the modeled and the measured values at 2cm is noticed, while a higher difference is observed at 4cm. The relative humidity differences ΔRH at 2 cm during the transient phase and during quasi steady state are evaluated at 4% and 7% respectively, while at 4 cm the ΔRH was evaluated at 5% and 13% respectively. This means that the relative humidity differences are larger than the sensor's uncertainty (3.5%), especially at 4 cm. These differences can be explained by sensors' sensitivities, sensors' position, humidity infiltrations, and the imperfect symmetric loads between T and φ at both faces of the samples, as well as the high heterogeneity of the media.

Fig. 14 presents the mean moisture content evolution versus time. The sorption stage starts from 8.5 kg/kg which is in agreement with the sorption and desorption test results shown in Fig. 2. The differences observed between the measured and the modelled water content are evaluated to 10% and 15% at 2cm and 4 cm respectively. In order to reach more accuracy of water content evolution model within wood fiber, a hysteresis model will be the subject of the forthcoming studies.

5 Uncontrolled conditions test

5.1 Experimental setup and boundary conditions

After testing the hygrothermal behavior of the wood fiber material under controlled conditions in the laboratory, where different ambient conditions were generated inside a climatic chamber, the fiber wood sample was inserted in the laboratory wall, in the ventilation opening, as illustrated in Fig. 15. The same sample was reused in order to keep the same material's properties, sensor's position and avoid all disturbances of initial water content. This study was done during the month of March.

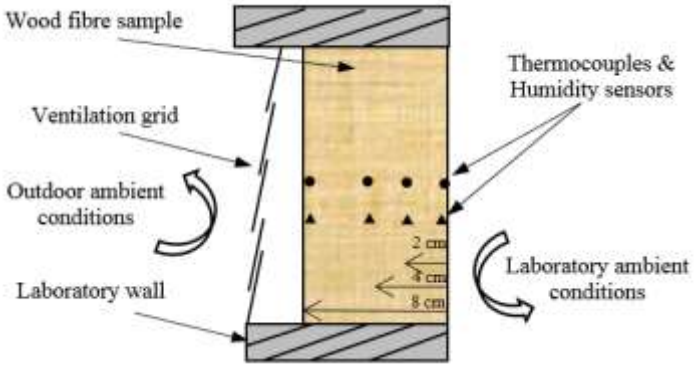

Figure 15- Vertical cross section of the test under uncontrolled conditions

The test of wood fiber under uncontrolled conditions lasted for two weeks; the external face was protected with a metal ventilation grid device preventing the rainwater infiltration disturbance. The measurements of ambient relative humidity and temperature at the interior and exterior interfaces of the sample are reported in Fig. 16. The curves' continuity proves the proper installation of the sample within the wall, the airtightness, and the high stability of the sample's state. A more or less constant value of the internal ambient conditions is observed with an internal air temperature mean value of 16,81°C ± 0,67°C and an internal air relative humidity of 38,92% ± 2,5%. On the external side, a quasi-sinusoidal cyclic profile was observed for both temperature and humidity variations with a 24h repetition period. The maximum and minimum external temperature values were evaluated at 20°C and 5,4°C respectively while the external humidity grows until 92,02% and goes down to 42,36%.

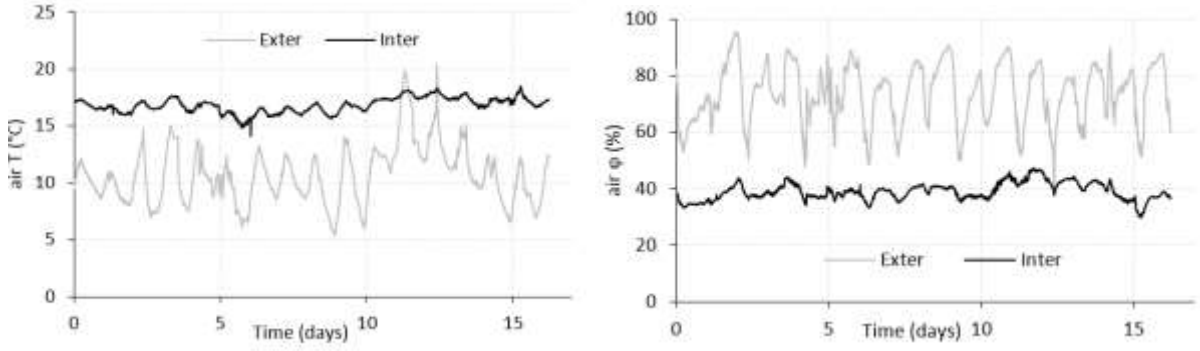

(a) (b)

Figure 16- Internal and external measured temperature (a) and relative humidity (b)

5.2 Experimental and numerical results

The modelling of the hygrothermal behavior of fiber wood insulation in the real ambient conditions aims to predict the hygrothermal behavior in real complex conditions. The measured and modelled results obtained for this case study are represented in Fig. 17 and Fig. 18 showing the measured and modelled temperature and relative humidity evolutions within the sample at x =2cm and 4cm.

A very high accordance is observed between these profiles. Regarding the temperature evolution (Fig. 17); a perfect correspondence is found at x = 4cm where the mean difference $\overline{\Delta T}$ is evaluated to 0,21°C, while $\overline{\Delta T}$ is estimated to 1°C at x = 2cm.

The maximum recorded differences for the relative humidity are: 5,5% and 4,5% at x = 2cm and 4 cm respectively.

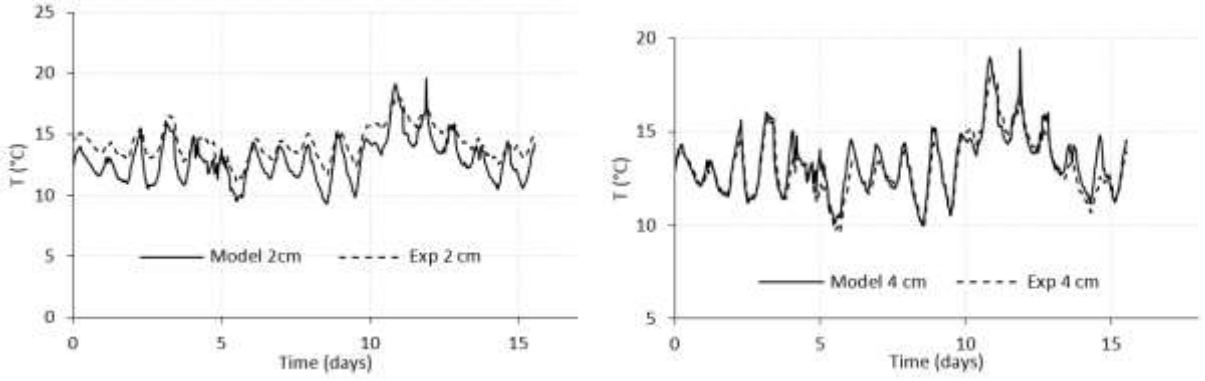

(a) (b)

Figure 17- Measured and modelled Temperature evolution at x = 2 cm (a) and x = 4 cm (b)

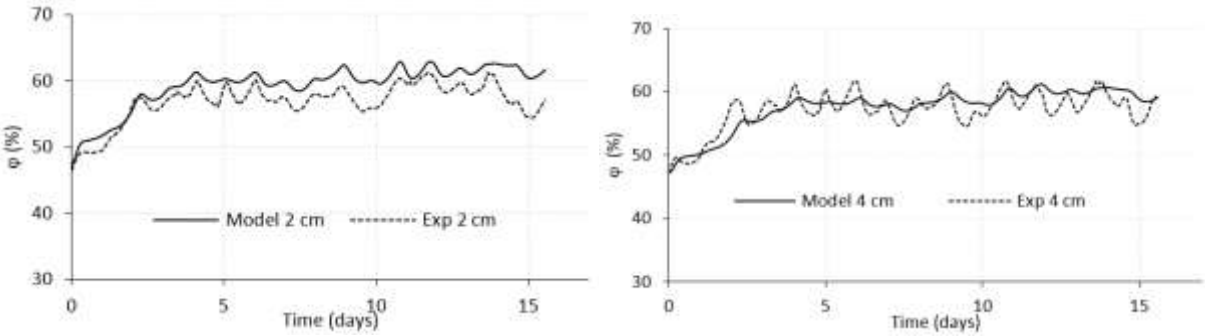

(a) (b)

Figure 18- Measured and modelled Relative humidity evolution at x = 2 cm (a) and x = 4 cm (b)

The time lags represent the response time difference between the outside and the generated inside peaks of temperature or humidity, while the decrement factor represents the amount by which the temperature or humidity peak is reduced by the time it reaches the inner surface **[52]**. An efficient building material is defined as one having a large time lags and a low decrement factor. The mean time lag and the mean decrement factor at 4 cm and 2 cm (depth of 6cm from external side) for relative humidity and temperature respectively are determined and represented in Fig. 19.

Promising result were found for relative humidity oscillations for the time lags (13h15 and 10h40) and the decrement factor (31,53% and 30,30%) at 2 cm and 4 cm (Fig. 19a).

The temperature results presented in Fig. 19b show that the time lag and decrement factor at 2 cm and 4 cm are respectively 02h55, 02h05, 11,45 % and 4,58%. These results are close to those presented by Rafidiarison et al [16] where they found a time lag of 3h00 for an 80 mm wood fiberboard sample having a 150 kg/m^{3}density. The wood fiber insulation material can thus be considered as an efficient material in term of moderation against external solicitation.

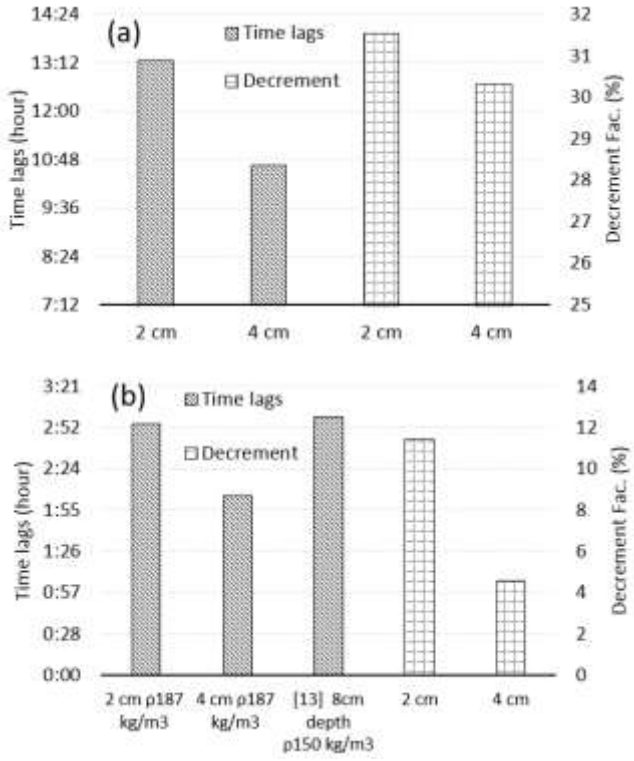

Figure 19- Mean time lags and decrement factor histogram for both relative humidity (a) and temperature (b) respectively

6 Sensitivity analysis

The slight observed differences between the experimental and numerical data in this study are principally due to the uncertainty of the sensors' position. Indeed, the installation of the sensors is very tricky; for this reason, a sensitivity study is presented below in order to quantify the sensors' position impact on the accuracy of the results.

The sensitivity study aims to evaluate the impact of the input parameters of the mathematical model describing the hygrothermal behavior of fiber wood. The approach is based on the determination of a sensitivity index, calculated as the relative deviation between the variation of output model functions compared to reference functions. The relative deviation is calculated according to the Eq. 18.

$$\delta_r = \frac{|x_{sim} - x_{ref}|}{x_{ref}} \text{ x } 100 \quad (18)$$

Where δ_r represents the relative deviation, x_{sim} is the output function with parameter variation, and x_{ref} is the reference function.

In order to evaluate the uncertainty of the sensor's position, a variation of ±5mm within the sample at 4cm was considered.

Fig. 20 represents the sensitivity profiles computed using Eq. 18 for the temperature and the relative humidity, induced by a perturbation of ±5mm of the sensor's position in the middle of the sample. We observe that the average values of temperature profile are - 2,93 % and - 2,90 % of relative humidity. According to these curves we can deduce that, for each 5mm uncertainty of the sensor's position, we obtain nearly 3% of errors between the simulated and measured data.

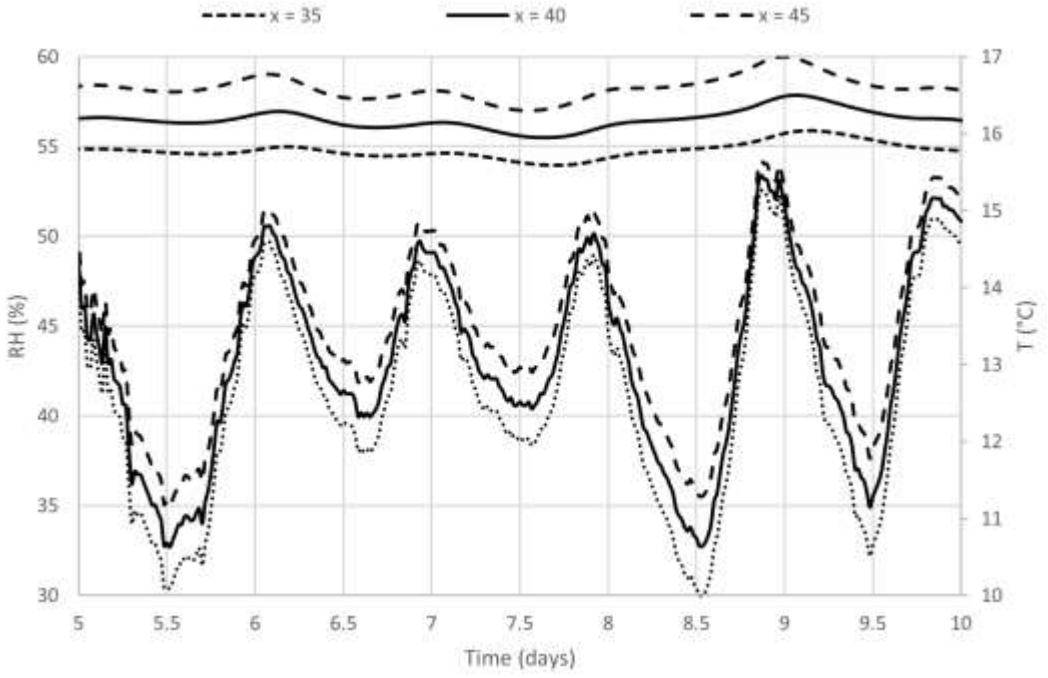

Figure 20- Temperature and relative humidity evolution at different positions within sample 35mm, 40mm, 45mm

7 Conclusions

This work investigated the hygrothermal behavior of wood fiber insulation both experimentally and numerically. The mathematical model of Philip and De Vries **[24]**, describing heat and mass transfer in porous media, was adopted for this bio-based material having a complex structure.

The water vapor sorption curve was first determined to know the studied material reaction against the micro-climatic conditions and represent the hygroscopic map of the material.

The thermophysical and hygroscopic properties were determined through experimental characterization methods according to the standards in order to simulate the material behavior in real conditions. An increasing thermal conductivity between 0.045 $W.m^{-1}.K^{-1}$ and 0.06 $W.m^{-1}.K^{-1}$ was found for a water content increasing from 2% to 18%. Similarly, the volumetric heat capacity had an

increasing shape varying between 250 000 $J.m^{-3}.K^{-1}$ and 350 000 $J.m^{-3}.K^{-1}$ for the same water content range.

Then, a representative wood fiber sample was subjected to different ambient conditions and instrumented with thermocouples and humidity sensors. The numerical model of Philip and De Vries [24] was implemented in Comsol Multiphysics® [34] using measured air temperature and air relative humidity at the interface as boundary conditions and compared to experimental measurements in controlled and uncontrolled ambiances.

Three controlled boundary scenarios were considered:

- In the first protocol, the transient relative humidity was studied by maintaining the temperature constant.
- In the second protocol, the relative humidity was maintained constant and the transient temperature was imposed.
- In the third protocol, a coupling of the air temperature and humidity ambient variations was studied.

A general good agreement was recorded between the simulated and the measured temperatures and relative humidity in the three protocols which validates the wood fiber behavior under controlled conditions.

The sample was then tested under uncontrolled conditions in order to predict the hygrothermal behavior of the wood fiber in real ambient conditions.

A very high accordance is observed between the measured and modelled results for both the temperature and the relative humidity evolutions within the sample with a maximum difference of less than 5,5% for the relative humidity, and a maximum difference of 0.21°C for the temperature profiles.

The obtained results highlight the coupling effect between the heat and mass transfer inside bio-based materials and allow the validation of the mathematical model describing heat and mass transfer within the wood fiber insulation material in stochastic real ambient conditions.

Both numerical and experimental approaches can be improved to predict the hygrothermal behavior of wood fiber with higher accuracy. More characterization series can be done, such as water vapor permeability determination or porosity analysis, to better understand the wood nature. The hysteresis models describing the isothermal of sorption and desorption is also foreseen in previous studies.

Acknowledgment

This work is done as part of the project “Projet citoyen P2AR” financed by the region Nord Pas de Calais, France.

Conflict of interest

The authors declare that they have no known competing financial interests or personal relationships that could have appeared to influence the work reported in this paper.

References

[1] http://www.cop21.gouv.fr/.

[2] Convention-cadre sur les changements climatiques, Conférnce des parties, Paris, 30 novembre - 11 décembre.

[3] ADEM, http://www.ademe.fr/Bâtiment-chiffres-clés-2013.

[4] http://data.worldbank.org/indicator/.

[5] Oil price developments: drivers, economic consequences and policy responses, OECD Economic.

[6] K. Thomsen E. et al., Energy consumption and indoor climate in a residential building before and after comprehensive energy retrofitting, Energy and Buildings, pp. 8–16, Apr-2016.

[7] R. Holopainen, P. Tuomaala, P. Hernandez, T. Häkkinen, K. Piira, and J. Piippo, Comfort assessment in the context of sustainable buildings: Comparison of simplified and detailed human thermal sensation methods, Building and Environment, pp. 60–70, Sep-2013.

[8] K. Biswas, S. Shrestha, M. Bhandari S., and A. Desjarlais O., Insulation materials for commercial buildings in North America: An assessment of lifetime energy and environmental impacts, Energy and Buildings, pp. 256–269, Dec-2016.

[9] T. Khadiran, M. Hussein H., Z. Zainal, and R. Rusli, Advanced energy storage materials for building applications and their thermal performance characterization: A review, Renewable and Sustainable Energy Reviews, pp. 916–928, Dec-2015.

[10] C. Bories, E. Vedrenne, A. Paulhe-Masso, G. Vilarem, and C. Sablayrolles, Development of porous fired clay bricks with bio-based additives: Study of the environmental impacts by Life Cycle Assessment (LCA), Construction and Building Materials, pp. 1142–1151, Aug-2016.

[11] F. Bennai, N. Issaadi, K. Abahri, R. Belarbi, A. Tahakourt, Experimental characterization of thermal and hygric properties of hemp concrete with consideration of the material age evolution, Heat and Mass Transfer, vol. 54, pp. 1189–1197, 2018.

[12] N. Chennouf B. Agoudjil, A. Boudenne, K. Benzarti, F. Bouras, Hygrothermal characterization of a new bio-based construction material: Concrete reinforced with date palm fibers, Construction and Building Materials, vol. 192, pp. 348-356, 2018.

[13] V. Kočí, M.Jerman, Z. Pavlík, J. Maděra, J. Žák, R. Černý, Interior thermal insulation systems based on wood fiberboards: experimental analysis and computational assessment of hygrothermal and energy performance in the Central European climate, Energy and Buildings, vol.222, no. 110093, 2020.

[14] M.Li, V.Nicolas, M.Khelifa, M.El Ganaoui, V.Fierro, A.Celzard, Modelling the hygrothermal behaviour of cement-bonded wood composite panels as permanent formwork, Industrial Crops and Products, Volume 142, no. 111784, 2019

[15] D. Taoukil, A. bouardi, F. Sick, Mimet A., Ezbakhe H., and Ajzoul T., Moisture content influence on the thermal conductivity and diffusivity of wood–concrete composite, Construction and Building Materials, pp. 104–115, 2013.

[16] H. Rafidiarison, R. Rémond, and E. Mougel, Dataset for validating 1-D heat and mass transfer models within building walls with hygroscopic materials, Building and Environment, pp. 356–368, 14-Mar-2015.

[17] D. Lelievre, T. Colinart, and P. Glouannec, Hygrothermal behavior of bio-based building materials including hysteresis effects: Experimental and numerical analyses, Energy and Buildings, pp. 617–627, 07-Sep-2014.

[18] Mourad RAHIM, Analyse et caractérisation du comportement hygrothermique de parois agro-sourcées à l'échelle 1: expérimentation et modélisation, Université de Picardie Jules Verne, 2015.

[19] E. Troppová, J Tippner, R. Hrcka, Thermophysical properties of medium density fiberboards measured by quasi-stationary method: experimental and numerical evaluation, Heat Mass Transfer, vol. 53, pp. 115–125, 2017.

[20] R. El-Sawalhi, J. Lux, P. Salagnac, Estimation of the thermal conductivity of hemp based insulation material from 3D tomographic images, Heat and Mass Transfer volume 52, pp. 1559–1569, 2016.

[21] R. R. Mvondo, J. C. Damfeu, P. Meukam, Y. Jannot, Influence of moisture content on the thermophysical properties of tropical wood species, Heat and Mass Transfer, vol. 56, pp.1365–1378, 2020.

[22] E. Latifa, R.M.H. Lawrence, A.D. Shea, P. Walker, An experimental investigation into the comparative hygrothermal performance of wall panels incorporating wood fibre, mineral wool and hemp-lime, Energy and Buildings, vol. 165, pp. 76-91, 2018.

[23] D. M. Nguyen, A. Grillet, T. M. Diep, Q.Bui, M. Woloszyn, Characterization of hygrothermal insulating biomaterials modified by inorganic adsorbents, Heat and Mass Transfer, vol. 56, pp. 2473–2485, 2020.

[24] J. R. Philip and D. A. De Vries, Moisture Movement in Porous Materials under Temperature Gradients, Transactions, American Geophysical Union, pp. 222–232, Apr-1957.

[25] S. Whitaker, Simultaneous Heat, Mass, and Momentum Transfer in Porous Media: A Theory of Drying, Advances In Heat Transfer, 1977.

[26] A. V. Luikov, System of differential equation of heat and mass transfer in capillary porous bodies, International Journal of Heat and Mass Transfer, pp. 1–14, 1957.

[27] E. Samson, J. Marchand, and J. J. Beaudoinc, Describing ion diffusion mechanisms in cement-based materials using the homogenization technique, Cement and Concrete Research, pp. 1341–1345, Aug-1999.

[28] S. Maghous, Z. Saad, L. Dormieux, and J. Canou, A model for in situ grouting with account for particle filtration, Computers and Geotechnics, pp. 164–174, 2007.

[29] H. . Kunzel, Simultaneous heat and moisture transport in building components: one- and two dimensional calculation using simple parameters, IRB Verlag Suttgart, 1995.

[30] A. Fick, Ûber diffusion, Annalen der Physik und Chemie, v.94, pp. 59–86.

[31] T. Defraeye, B. Blocken, D. Derome, and B. Nicolai, Convective heat and mass transfer modelling at air–porous material interfaces: overview of existing methods and relevance, Chemical Engineering Science, pp. 49–58, 2012.

[32] A. Zaknoune, P. Glouannec, and P. Salagnac, Identification of the Liquid and Vapour Transport Parameters of an Ecological Building Material in Its Early Stages, Transport in Porous Media, pp. 589–613, 2013.

[33] C. Maalouf, A. D. Tran Le, S. B. Umurigirwa, M. Lachi, and O. Douzane, Study of hygrothermal behaviour of a hemp concrete building envelope under summer conditions in France, Energy and Buildings, pp. 48–57, 2014.

[34] Comsol Multiphysics, http://www.comsol.com/products/multiphysics/.

[35] J. Wallace, P. Hobbs, Atmospheric Science, Second Edition: An Introductory Survey (International Geophysics) 2nd Edition

[36] O. Vololonirina, M. Coutand, and B. Perrin, Characterization of hygrothermal properties of wood based products - Impact of moisture content and temperature, Construction and Building Materials, pp. 223–233, 2014.

[37] A. Limam, A. f Zerizer, D. Quenard, H. Sallee, and A. Chenak, Experimental thermal characterization of bio-based materials (Aleppo Pine wood, cork and their composites) for building insulation, Energy and Buildings, pp. 89–95, 2016.

[38] S. Geving, E. Lunde, and J. Holme, Laboratory investigations of moisture conditions in wood frame walls with wood fiber insulation, Energy Procedia, pp. 1455–1460, 2015.

[39] F. Collet, F. Achchaq, K. Djellab, L. Marmoret, and H. Beji, Water vapor properties of two hemp wools manufactured with different treatments, Constr. Build. Mater., vol. 25, no. 2, pp. 1079–1085, Feb. 2011.

[40] Reporting physisorption data for gas/solid systems with special reference to the determination of surface area and porosity, International Union of pure and applied chemistry, pp. 2201–2218, 1982.

[41] M. Donohue D. and G. Aranovich L., Adsorption Hysteresis in Porous Solids, Journal of Colloid and interface science, pp. 121–130, 17-Mar-1988.

[42] NF EN ISO 12571 Hygrothermal performance of building materials and products- Determination of hygroscopic sorption properties, 25-Oct-2013.

[43] Langmuir, The adsorption of gases on plane surfaces of glass, mica and Platinum, Journal of the American Chemical Society, pp. 1361–1403, 1918.

[44] E. Guggenheim, Application of statistical mechanics, Oxford University Press, 1966.

[45] R. Anderson, Modifications of the brunauer, Emmett and teller, pp. 686–91, 1946.

[46] von H. J. de Boer., The Dynamical Character of Adsorption, Oxford University Press, 1953.

[47] S. EN BRUNAUE, P. EMMET, and E. TELLER, Adsorption of gases in miltimolecular layer, Contribution from the bureau of chemistry and sons and george washington university, pp. 309–319, Feb-1938.

[48] NF EN 12664, Thermal performance of building materials and products. Determination of thermal resistance by means of guarded hot plate and heat flow meter methods. Dry and moist products of medium and low thermal resistance, pp. 75–225, 2001.

[49] NF EN ISO 12572 Hygrothermal performance of building material and products- Determination of water vapour transmission properties, Oct-2001.

[50] Chamoin, Optimisation des propriétés (physiques, mécaniques et hydriques) de bétons de chanvre par la maîtrise de la formulation, INSA de Rennes, 2013.

[51] http://graphteccorp.com/instruments/gl82/index.html.

[52] H. Asan and Y. Sancaktar, Effects of Wall's thermophysical properties on time lag and decrement factor, Energy and Buildings, pp. 159–166, Jun-1997.